Desalination and Water Treatment
www.deswater.com

doi: 10.5004/dwt.2018.22986

130 (2018) 132–141
October

Adsorption of cationic dye using novel O-amine functionalized chitosan Schiff base derivatives: isotherm and kinetic studies

Ahmed Shebl[a,*], A.M. Omer[b], T.M. Tamer[b]

[a]*Chemistry Department, Faculty of Science, Ain Shams University, Abbassia 11566, Cairo, Egypt, email: a_ahmed@sci.asu.edu.eg*
[b]*Polymer Materials Research Department, Advanced Technologies and New Materials Research Institute (ATNMRI), City of Scientific Research and Technological Applications (SRTA-City), New Borg El-Arab City, P.O. Box: 21934, Alexandria, Egypt, emails: ahmedomer_81@yahoo.com (A.M. Omer), ttamer85@yahoo.com (T.M. Tamer)*

Received 17 January 2018; Accepted 25 August 2018

ABSTRACT

New Schiff bases of O-amine functionalized chitosan derivatives were obtained from the coupling of O-amine functionalized chitosan with 4-methoxy benzaldehyde (Schiff base I), 4-chloro benzaldehyde (Schiff base II), and diethyl amino acetone (Schiff base III). The structure of the prepared innovative Schiff bases was characterized using Fourier transform infrared, thermal gravimetric analysis, differential scanning calorimetry, and scanning electron microscope. A batch system was applied to study the adsorption of methylene blue (as a model of cationic dye) from aqueous solutions using these new Schiff bases. The adsorption parameters were studied and recorded for prepared derivatives as: pH 7, 250 rpm, and time 40, 120, and 180 min for Schiff bases (I), (II), and (III), respectively. And the maximum adsorption capacity was recorded as 35.6, 25.79, and 30.51 mg/g for the same sample order. The equilibrium adsorption data of reactive dye on O-amine functionalized chitosan derivatives were analyzed by Langmuir and Freundlich models. The Freundlich model represents the experimental data better that Langmuir one (with R^2 (I) = 0.9807, R^2 (II) = 0.983, and R^2 (III) = 0.9994). The kinetic adsorption data were analyzed using four different kinetic models: pseudo-first-order, pseudo-second-order, intraparticle diffusion, and Avrami models. Obtained results were more fit to pseudo-second-order model (with R^2 (I) = 0.9970, R^2 (II) = 0.9968, and R^2 (III) = 0.9995).

Keywords: Wastewater treatment; Adsorption; Cationic dye; Chitosan Schiff base; Isotherm model; Kinetic model

1. Introduction

Contamination of water with colored pollutants such as dyes is mainly originated from some industries such as textile, leather, and plastics. A microscopic amount of dye in fresh water is highly visible and toxic to living creatures of aquatic habitat as well as to human beings. Therefore, the elimination of dyes from waste effluents is environmentally necessary.

Several methods were employed for dye removing including adsorption process, oxidation–ozonation process, biological treatment, coagulation–flocculation system, and membrane separation [1]. Among several chemical and physical systems, adsorption is one of the favorable methods for dye removal from both environmental and economic point of views. Various low-cost adsorbents have been suggested and investigated for their capacity to remove dyes [1–6]. Recently, specific interest has been directed to utilize natural materials in this proposal [7–10] and also natural polysaccharide-based adsorbents such as chitin and its derivatives [11,12].

Chitin is the second most abundant polysaccharide next to cellulose. Chemically, it consists of β-(1–4)-2-*N*-acetyl-2-deoxy β-d-glucopyranose repeating unit [13,14]. Chitosan

* Corresponding author.

1944-3994/1944-3986 © 2018 Desalination Publications. All rights reserved.

is the primary derivative of chitin, prepared by its partial deacetylation. The free amine groups (–NH_2) located along the polymer backbone is responsible for its basic character, making it suitable for different applications such as water treatment [15], antibacterial [16], antifungal [17], antioxidant [18,19], drug delivery [20–22], and medical applications [23].

Regarding water treatment application, chitosan is considered a suitable candidate for anionic dye adsorption rather than cationic one [24–28] especially at lower pH values, since the free amine groups become protonated and attain positive charges that are responsible for strong electrostatic attraction with anionic dye molecules.

Chitosan Schiff base derivatives are common derivatives of chitosan prepared by interaction of chitosan amine groups with carbonyl group of aldehydes and ketones to form corresponding azomethine derivatives (C=N linkage). Chitosan Schiff base derivatives have been prepared and widely used for water purification application as dye and heavy metal removal [29–32].

In this study, new Schiff base derivatives of chitosan were prepared, characterized, and evaluated as adsorbents for methylene blue (MB) – as a model of cationic dye – relying on their new acquired features. The high affinity of prepared derivatives against cationic dye was recorded at neutral and alkaline pH. Since the immobilization of phenolic Schiff bases along the backbone of chitosan derivatives shows high affinity of absorbent to cationic dyes. That enhances the activity of chitosan as cationic polymer to be suitable for removing both cationic and anionic dyes.

2. Materials and methods

2.1. Materials

O-amine functionalized chitosan was previously prepared in our laboratory [18]. Acetic acid (99.8%), hydrochloric acid (37%), sodium hydroxide pellets (99%–100%), MB, 4-methoxy benzaldehyde, 4-chloro benzaldehyde, and diethylamino acetone were all purchased from Sigma-Aldrich (Germany) and used without further purification.

2.2. Methods

2.2.1. Preparation of O-amine functionalized chitosan Schiff bases

O-amine functionalized chitosan Schiff bases were prepared by modification of Soliman et al. [33] method. In detail, 1 g of the O-amine functionalized chitosan was dissolved in 200 mL acetic acid solution (2%) at ambient temperature overnight. Filtration of O-amine functionalized chitosan solution was carried out using cheesecloth to remove undissolved chitosan. Then a certain amount of absolute ethanol was added to O-amine functionalized chitosan solution, with continuous stirring to have a homogenous solution. 31 mmol of 4-methoxy benzaldehyde, 4-chloro benzaldehyde, or diethylamino acetone that was previously dissolved in 20 mL ethanol was added to the above solution. After that, the temperature was raised to 80°C and the reaction mixture was left to react under continuous stirring for 3 h. The obtained gels were collected by filtration, washed several times with ethanol to remove any unreacted aldehydes or ketones, and finally dried at 60°C under reduced pressure.

2.2.2. Characterization

2.2.2.1. Infrared spectral analysis Functional groups of O-amine functionalized chitosan Schiff bases were confirmed using Fourier transform infrared spectrophotometer (Shimadzu FTIR – 8400S, Japan). 1–2 mg of samples were milled with 200 mg previously dried KBr and pressed to discs at 10 bar. The transmission of samples was recorded from 400 to 4,000 cm^{-1}.

2.2.2.2. Thermal gravimetric analysis Thermal gravimetric analysis (TGA) of the samples under study was carried out using thermogravimetric analyzer (Shimadzu TGA–50, Japan) under nitrogen atmosphere to evidence the changes in structure as a result of the modification. The weight loss of the samples was first measured starting from room temperature to 120°C at a heating rate of 10°C/min. Then, the samples were cooled and reanalyzed from room temperature to 600°C.

2.2.2.3. Differential scanning calorimetry Differential scanning calorimetric (DSC) analysis was carried out by means of differential scanning calorimeter (Shimadzu DSC–60-A, Japan) under nitrogen atmosphere with a flow rate of 30 mL/min. The temperature was raised from ambient to 350°C with a rate of 10°C/min.

2.2.2.4. Scanning electron microscopic analysis Samples were coated under vacuum with a thin layer of gold before being examined by scanning electron microscopy (SEM). Morphological changes of the samples surface were followed using SEM (Joel Jsm 6360LA), Japan.

2.2.3. Batch equilibrium studies

The stock solution of 1 g/L of MB dye (1,000 ppm) was prepared by dissolving the appropriate amount of dye in distilled water then the used concentrations were obtained by dilution. All the adsorption experiments were conducted in 100 mL flasks by adding a given amount of adsorbent to 25 mL dye solution of different concentrations with different pH values and shaking in an orbital shaker for a given time. The adsorbate concentrations in the initial and final aqueous solutions were measured using UV-Vis spectrophotometer at 664 nm. The amount of dye adsorbed was calculated from the difference between the initial concentration and the equilibrium one. The values of percentage removal and the amount of dye adsorbed were calculated using the following relationship:

$$\text{Dye removal}\,\% = \frac{\left(C_o - C_e\right)}{C_o} \times 100 \quad (1)$$

where C_o is the initial dye concentration and C_e is the final dye concentration in supernatant at equilibrium.

2.2.4. Adsorption isotherm models

The adsorption isotherms get their beneficial use from their applicability to describe the interaction between the

adsorbate and the adsorbent of a given system. Several models can be used to analyze the experimental data to provide information about the adsorption mechanism as well as the adsorbent surface properties and affinities. The most accepted models for single solute systems are Freundlich and Langmuir models [34–36].

The linear form of Freundlich equation can be presented as follows:

$$\log q_e = \log K_F + \frac{1}{n_F} \log C_e \tag{2}$$

where q_e is the equilibrium adsorption capacity which is the amount of adsorbed molecules per gram of adsorbent at equilibrium (mg/g), C_e is the solution equilibrium concentration (mg/L), K_F and n_F are the Freundlich parameters that represented the adsorbent affinity ((mg/g)(L/mg)$^{1/n}$) and the heterogeneity factor, respectively. These parameters can be obtained from the intercept and slope of the straight line of the plot log q_e against log C_e.

On the other hand, the linear form of Langmuir equation can be expressed as follows:

$$\frac{C_e}{q_e} = \frac{1}{K_L} + \frac{a_L}{K_L} C_e \tag{3}$$

where K_L and a_L are Langmuir constants that can be obtained from the intercept and slope of the straight line of the plot C_e/q_e versus C_e. The a_L constant is related to the free energy or net enthalpy of adsorption (L/mg) ($a_L \propto e^{-\Delta H/RT}$), whereas K_L is the equilibrium constant of Langmuir (L/g). The constant q_{max} which equals K_L/a_L (mg/g) is the monolayer saturation capacity representing the maximum adsorption capacity of the adsorbent for a given adsorbate.

The experimental data of the adsorption isotherm for our systems were analyzed by linear fitting to both models.

2.2.5. Adsorption kinetics

Kinetic of the adsorption process is vital to understand the dynamics of the adsorption reaction in terms of the order and the rate constant. Therefore, pseudo-first-order (Lagergren model), pseudo-second-order, intraparticle diffusion (Webber and Morris model) and Avrami kinetic models were utilized in this study.

Their linear equations are presented as follows:

Pseudo-first-order $$\ln(q_e - q_t) = \ln q_e - k_1 t \tag{4}$$

Pseudo-second-order $$\frac{t}{q_t} = \frac{1}{k_2 q_e^2} + \frac{t}{q_e} \tag{5}$$

Intraparticle diffusion $$q_t = k_i \sqrt{t} \tag{6}$$

Avrami $$\ln\left\{\ln\left(\frac{q_e}{q_e - q_t}\right)\right\} = n_{AV} \ln k_{AV} + n_{AV} \ln t \tag{7}$$

where k_1 is the pseudo-first-order rate constant (min^{-1}), k_2 is the pseudo-second-order rate constant (g/mg/min), k_i is the intraparticle diffusion model rate constant (mg/g/min$^{0.5}$), k_{AV} is the Avrami kinetic rate constant (min^{-1}), and n_{AV} is the Avrami exponential.

The experimental data of the adsorption kinetics for our systems were analyzed by linear fitting of these four models.

3. Results and discussions

The ease of chemical transformation of chitosan and its O-amine functionalized derivatives is supported by the presence of amine groups along the polymer chains. The reaction of free amino groups with active carbonyl compounds such as aldehyde or ketone to give Schiff bases is considered the easiest transformation [15,16,37]. The resulted (–RC=N–) groups of these Schiff bases exhibit significant analytical and environmental applications via improving the adsorption/complexation properties [38]. In current work, three Schiff bases were synthesized by coupling O-amine functionalized chitosan with of 4-methoxy benzaldehyde, 4-chloro benzaldehyde, and diethylamino acetone to give Schiff bases (I), (II), and (III), respectively (Fig. 1).

3.1. Characterization

3.1.1. Fourier transform infrared

Fig. 2(a) illustrates FTIR spectra of O-amine functionalized chitosan Schiff base derivatives. Two strong NH_2 stretching bands are observed, asymmetric stretching at 3,360–3,340 cm^{-1} and symmetric stretching at 3,190–3,170 cm^{-1}, which are due to primary amides (–CO–NH–). They also exhibit C=O stretching at 1,680–1,660 cm^{-1} (denoted as the amide I band) and NH_2 bending at 1,650–1,620 cm^{-1} (denoted as the amide II band). Secondary amides display an N–H stretching band at 3,300–3,250 cm^{-1}, while the carbonyl stretching (amide I band) is noticed at 1,680–1,640 cm^{-1}. The amide II band for secondary amides appears at 1,560–1,530 cm^{-1} is attributed to the coupling of N–H bending and C–N stretching. Bands between 2,850 and 2,950 cm^{-1} are a combination of C–H stretching of methyl and methylene groups, while band at 1,630–1,650 cm^{-1} as well as bands between 1,400 and 1,600 cm^{-1} are ascribed to stretching vibration of C=C and aromatic C=C, respectively. Bands at 1,020 cm^{-1} point out to C–O–H group stretching. A characteristic band at 870 and 815 cm^{-1} for Schiff base (I) and (II), respectively, is attributed to 1, 4 aromatic substitution.

3.1.2. Thermal gravimetric analysis

Fig. 2(b) represents the TGA of the three Schiff bases under study. Generally, chitosan derivatives represent three different degradation stages; the first stage starts from ambient temperature up to 150°C with weight loss 8.9%–9.1% as a result of the elevation of moisture content that is associated with polymer chains. Next degradation stage refers to thermal destruction of pyranose ring. The main thermal process of the prepared polymers takes place at various temperatures; 242°C–296°C (21.73%) for Schiff base (I), 261°C–312°C (21.62%) for Schiff base (II), and 253.51°C–317°C (25.54%) for

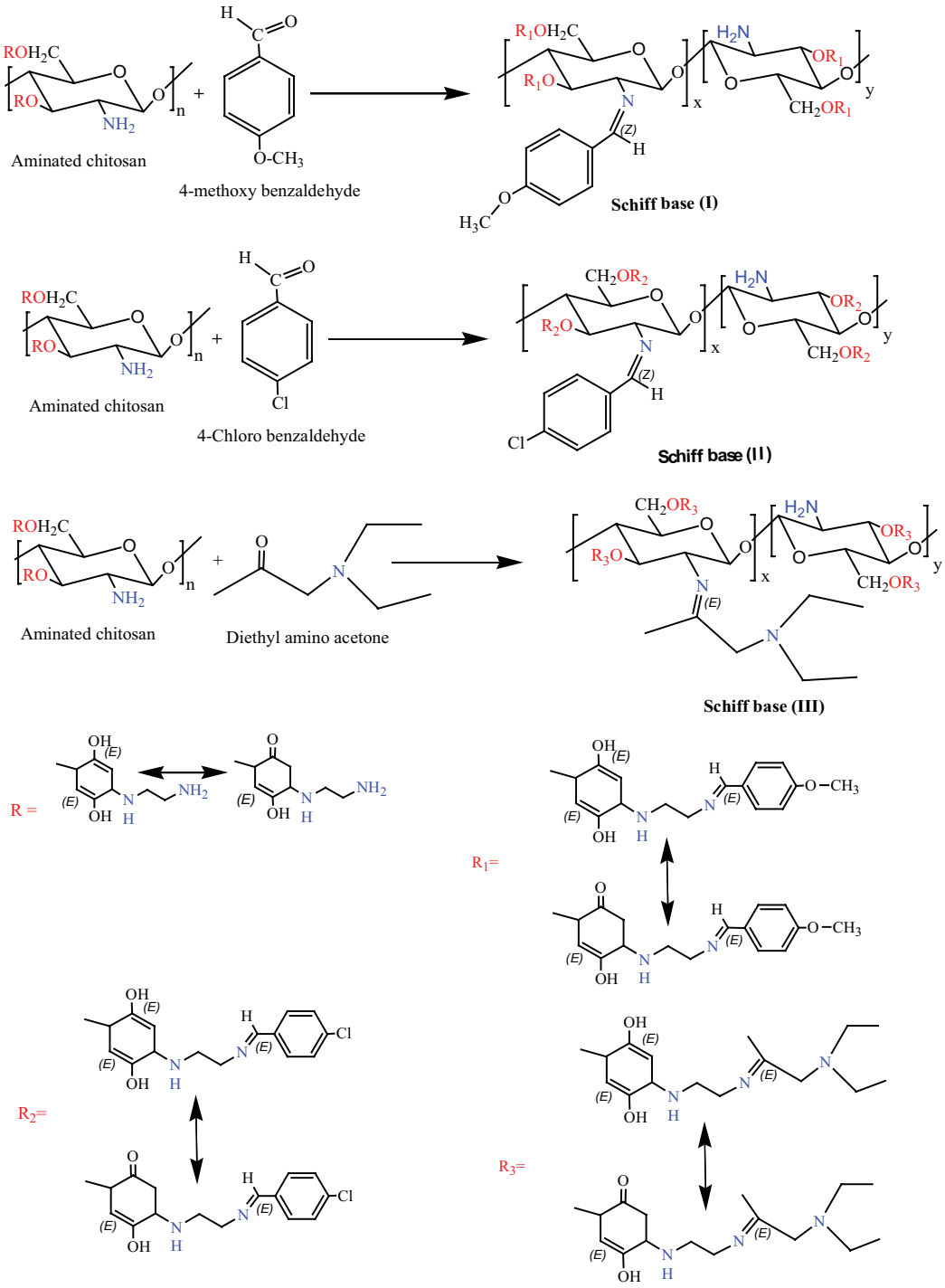

Fig. 1. Schematic preparation routes of Schiff bases (I), (II), and (III).

Schiff base (III). That is indicating Schiff base (II) is the highest thermally stable one whereas Schiff base (I) is the lowest.

3.1.3. Differential scanning calorimetry

DSC curves of the three Schiff bases (I), (II), and (III) are shown in Fig. 2(c). Broad endothermic peaks are recognized starting from ambient temperature to 90°C that is corresponding to loss of polymer moisture content. Chart exhibits polymer glassy transition temperature at 95°C, 118°C, and 117°C for Schiff bases (I), (II), and (III), respectively. The second thermal event may be related to the decomposition of glucose amine (GlcN) units with correspondence exothermic peak at 268°C,, 286°C, and 296°C for Schiff bases (I), (II) and (III), respectively.

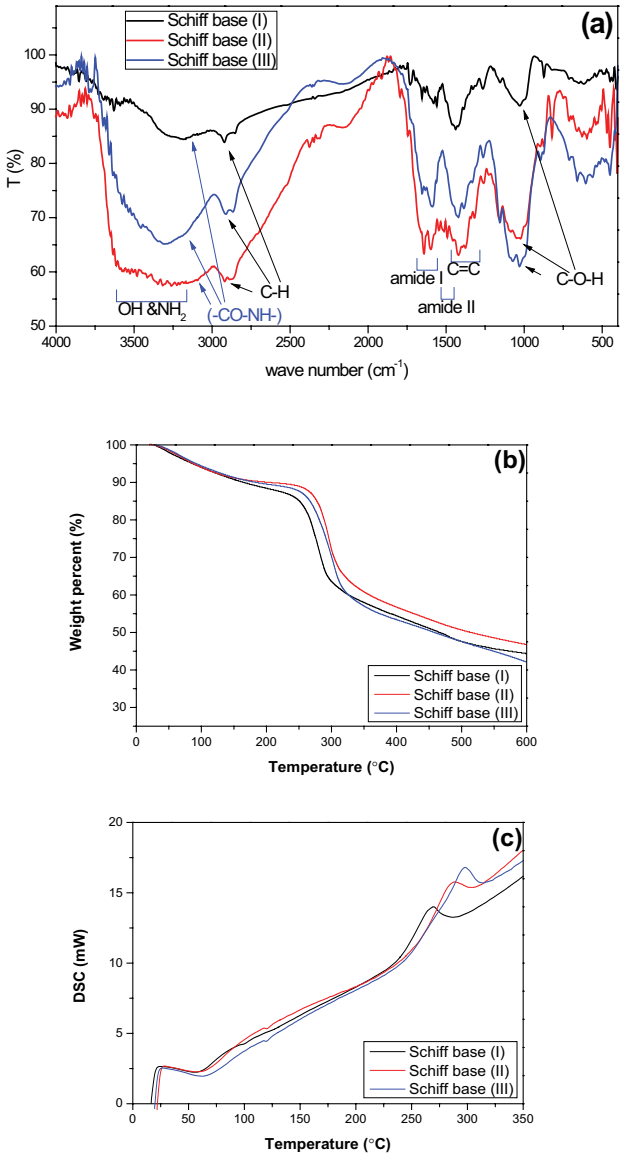

Fig. 2. (a) FTIR spectra, (b) thermal gravimetric analysis, and (c) differential scanning calorimetric measurements of Schiff bases (I), (II) and (III).

3.1.4. Scanning electron microscope

The surface morphology of O-amine functionalized chitosan Schiff bases (I), (II), and (III) was investigated by SEM and presented in Fig. 3. The SEM images showed a rough surface with a microporous structure for all tested samples. Formulation of the crystal structure of chitosan is controlled by its functional groups (hydroxyl and amine groups). Modification of polymer generates new functional groups which may distort its microstructure. In current structures, some of the amine groups were coupled with hydrophobic aldehyde/ketone to form the corresponding Schiff bases. The combination of hydrophilic–hydrophobic groups along polymer backbone can explain the rough and porous structure of chitosan derivatives. The pores are useful in increasing the working surface in the Schiff bases which enabled them to be used as promising adsorbents.

3.2. Batch adsorption experiments

The batch system model was employed to study the adsorption capacity of the MB dye of prepared Schiff bases (I, II, and III). The different parameters controlling the adsorption process was studied to release the optimum condition. The UV spectrum of MB solution before and after the removal process is presented in Fig. 4.

3.2.1. Effect of contact time

Fig. 5(a) shows the removal percent of MB dye on Schiff bases (I), (II), and (III) as a function of time, with the initial dye concentration taken = 25 ppm, adsorbent dose = 0.05 g, solution volume = 25 mL, temperature = 20°C ± 2°C, agitation rate = 200 rpm, and solution pH = 7. The chart shows an increase in dye removal with time and achieves equilibrium within 40, 120, and 180 min for Schiff bases (I), (II), and (III), respectively. Beyond this period, adsorption process is going to be in Plato region. The figure displays an improvement in the removing capacity of Schiff base (I) rather than Schiff bases (II) and (III) that can be ascribed to its higher electron density. Same trend was observed by adsorption of MB on chitosan-*g*-poly (acrylic acid)/vermiculite hydrogel composites [39] and chitosan hydrogel beads [40].

Adsorption of dye on chitosan derivatives is controlled by two parameters; the charged sites including hydrophilic

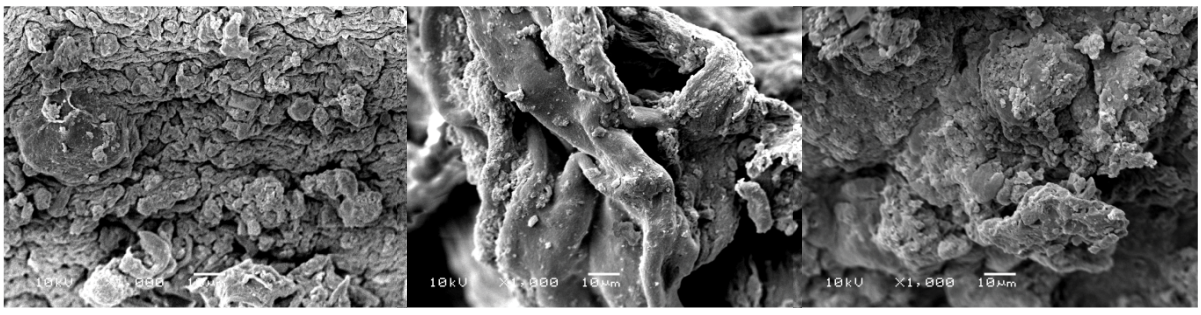

Schiff base (I) **Schiff base (II)** **Schiff base (III)**

Fig. 3. SEM images of Schiff bases (I), (II), and (III).

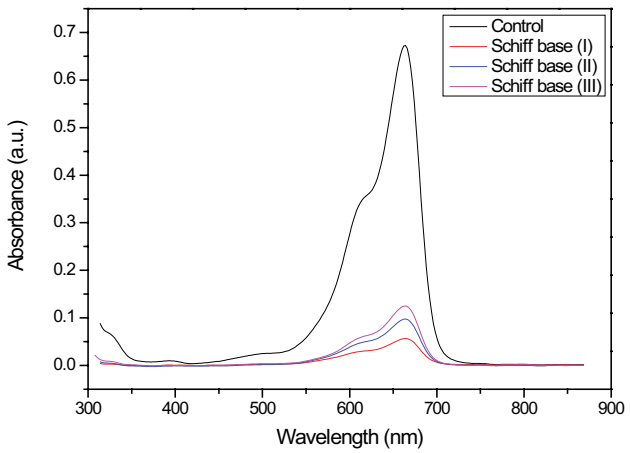

Fig. 4. UV spectrum of MB dye before and after adsorption process using Schiff bases (I), (II), and (III) (at equilibrium time, adsorbent dose = 0.05 g, solution volume = 25 mL, temperature = 20°C ± 2°C, agitation rate = 200 rpm, and solution pH = 7).

groups and hydrophobic interaction with methyl groups of glucose rings, acetyl groups and side chains of the Schiff base groups. For our derivatives, presence of reactive functional groups along polymer backbone such as OH, NH_2, C=N, in addition to the immobilized side chains, simplify its interaction with dye. These two factors are proposed in the competitive formation of both inter- and intramolecular H-bonds, as well as interactions with other substrates. Adsorption of cationic dye onto current chitosan derivatives was done via physical sorption behavior. Presence of high phenolic electron density of immobilized Schiff base groups enhances the adsorption affinity of polycationic polymers like chitosan to MB [15,41,42].

3.2.2. *Effect of initial dye concentration*

Effect of initial dye concentration of MB on adsorption process on O-amine functionalized chitosan Schiff bases was studied at optimum contact time 40, 120, and 180 min for Schiff bases (I), (II) and (III), respectively, with constant adsorption parameters of adsorbent dose = 0.05 g, solution volume = 25 mL, temperature = 20°C ± 2°C, agitation

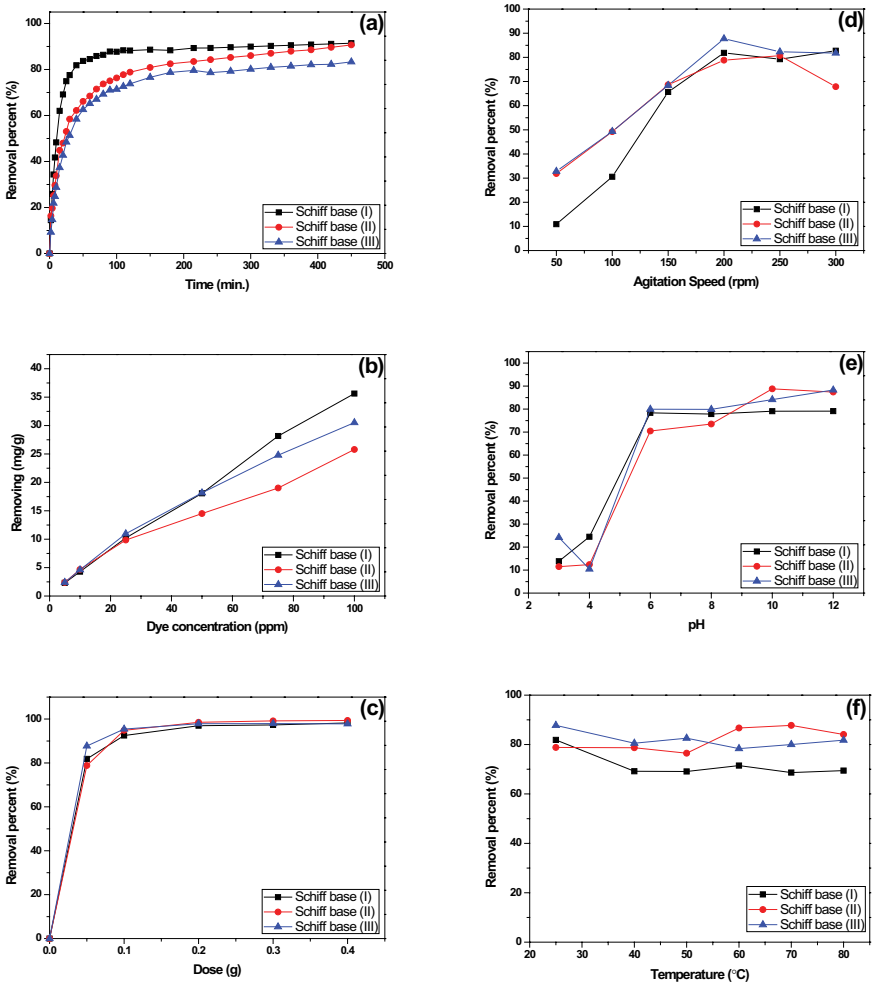

Fig. 5. Effect of (a) contact time, (b) initial dye concentration, (c) adsorbent dose, (d) agitation rate, (e) solution pH, and (f) solution temperature on the adsorption of MB by Schiff bases (I), (II), and (III).

rate = 200 rpm, and solution pH = 7, and presented in Fig. 5(b). The increase of dye concentration demonstrates a gradual increase in dye uptake. This indicates that the initial dye concentration plays a significant role in the adsorption capacities of O-amine functionalized chitosan derivatives toward MB. The dye particles could be attached to the available adsorption sites on the surface of the Schiff base molecules. This affinity of adsorbent to dye was enhanced at low dye concentration. On the other hand, by increasing the concentration, the dye molecules forced to adsorb on the less active side that led to a slower adsorption rate due to occupying of the several high energy adsorption sites [43].

3.2.3. Effect of adsorbent dose

Different amounts of O-amino functionalized Schiff bases varying from 0.05 to 0.4 g were used to study the effect of adsorbent dose on adsorption process. All measurements were equilibrated for the optimum time at an initial dye concentration of 25 ppm, solution volume = 25 mL, temperature = 20°C ± 2°C, agitation rate = 200 rpm, and solution pH = 7. The results are presented in Fig. 5(c). It is clear that the removal percent of MB was increased as adsorbent amount increased. This could be attributed to the fact that for the same initial dye concentration, increasing adsorbent amount provides greater surface area and sorption sites [42,44,45].

3.2.4. Effect of agitation rate on MB adsorption

The effect of agitation rate on the adsorption process was studied using different agitation rate from 20 to 300 rpm and presented in Fig. 5(d). All adsorption parameters were fixed at the optimum contact time, the initial dye concentration of 25 ppm, 0.05 g of absorbent, solution volume of 25 mL, temperature of 20°C ± 2°C at neutral pH. For all tested samples, there is an increase in adsorption process by increasing agitation rate up to 200 rpm. After that, the removing percent remains constant. Adsorption of dye on absorbent is influenced by a passive flow layer existing on the adsorbent surface. Increment in stirring rate causes an increase in film diffusivity. This improvement in film diffusivity facilitates dye diffusion, consequently increasing adsorption capacity. In addition, increase in the rate of stirring increases the probability of dye molecules to collide with absorbents' active sites [46,47]. Ruthven [48] suggested that intraparticle diffusivity value hugely depends on the surface properties of adsorbents and adsorption capacity.

3.2.5. Effect of solution pH

Environmental pH is a critical parameter that can alter the adsorption of dye molecules. Variation of pH value may affect the dissociation of functional groups on the active sites of the adsorbent and switching dye charges. Fig. 5(e) exhibits the effect of the pH value of artificial dye solutions on dye removal percent. The adsorption process was operated at optimum contact time, initial dye concentration = 25 ppm, adsorbent dose = 0.05 g, solution volume = 25 mL, temperature = 20°C ± 2°C, and agitation rate = 200 rpm. In overall, the dye uptakes are much lower at acidic pH than those in neutral and alkaline pH. That can be attributed to similarities of charges of dye and absorbent. At acidic pH, amine groups of Schiff bases are protonated producing positive charge along the polymer backbone. As test dye is a cationic dye, electrostatic repulsion force between dye and absorbent can prevent adsorption process. On the other hand, in neutral and alkaline pH, the surface charge of absorbent is switched so absorbents demonstrate a higher adsorption capacity. An appreciable amount of dye elimination in this pH range suggests physical adsorption through hydrogen bonding and Van der Waals forces that enhanced with presence of Schiff bases side chains [41].

3.2.6. Effect of solution temperature

Inference of environmental temperature on adsorption process was studied from 40°C to 80°C and presented in Fig. 5(f) (at the optimum contact time, initial MB concentration of 25 ppm, with the adsorbent dose of 50 mg/25 mL at neutral pH). By elevating the temperature, a slight increase in dye removal percent for Schiff base (II) is monitored whereas no significant change in case of Schiff bases (I) and (III) is observed.

The small improvement in the adsorption of MB on Schiff base (II) could be attributed to the swelling effect inside the internal structure of the adsorbent – that may be occurred by increasing the temperature – allowing the large dye molecules to penetrate and adsorb inside adsorbent [49].

3.3. Adsorption isotherm models

The analysis of the adsorption isotherm data obtained in this study for the three Schiff bases using different concentrations of MB was performed by fitting to the linear forms of both Freundlich and Langmuir models (Figs. 6(a) and (b), respectively). The values of Freundlich and Langmuir parameters, as well as the correlation coefficient (R^2), are shown in Table 1.

According to Freundlich model, which is empirical, the adsorbent surface can be regarded as a heterogeneous one in terms of possessing different adsorption sites energies [50,51]. On the other hand, Langmuir model mainly assumes that the adsorbent surface is homogenous, consisting of active sites that are equally available and energetically equivalent [52,53].

From Table 1, the values of R^2 of Freundlich model are much closer to 1.0 compared with those of Langmuir model, indicating that the Freundlich model represents the experimental data better than Langmuir one. This means that the adsorbent surface is heterogeneous which is supported by the fact that Schiff bases under study have different functional groups such as hydroxyl and amino ones as well as 4-methoxy benzyl, 4-chloro benzyl, and diethyl amino 2-propyl moieties for Schiff bases (I), (II), and (III), respectively. Those have different affinities for MB adsorption since they have different adsorption potentials [34]. The heterogeneity factor of the Schiff bases, n_F, has values between 1 and 10 implying that the adsorption process is favorable [54].

3.4. Adsorption kinetics

The kinetic adsorption data were analyzed using four different kinetic models: pseudo-first-order, pseudo-second-order, intraparticle diffusion, and Avrami models.

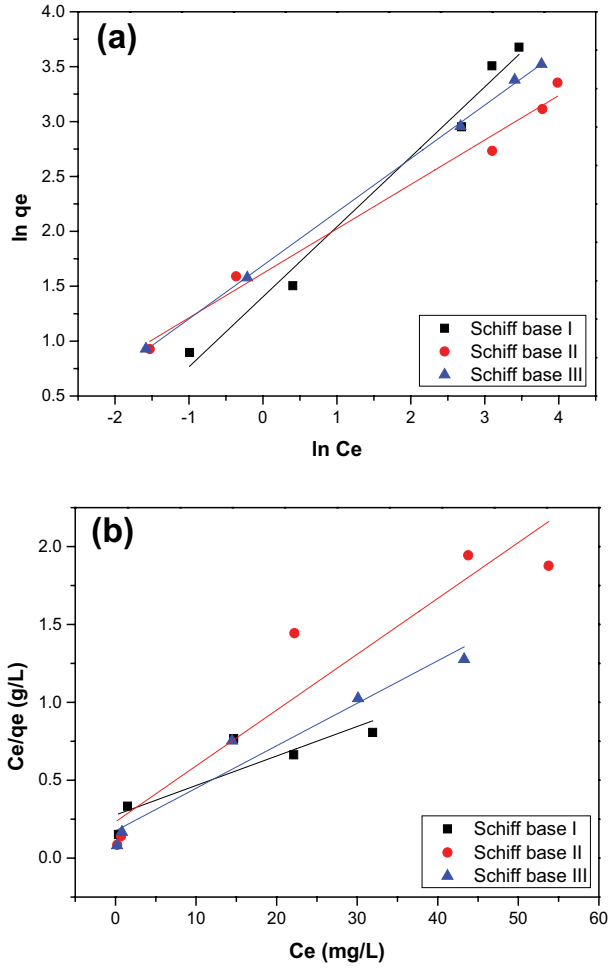

Fig. 6. Adsorption isotherm models of MB on the Schiff bases. (a) Freundlich model and (b) Langmuir model.

The pseudo-first-order model [55] (Lagergren model) is the earliest known equation expressing the adsorption rate depending on the adsorption capacity (i.e., controlled by adsorbate concentration). The pseudo-second-order model [56] suggests that the adsorption process may be controlled by chemisorption which involves valency forces through sharing or exchange of electrons between the adsorbent and the adsorbate.

The intraparticle diffusion model introduced by Ref. [57] describes that the process is diffusion controlled if its rate depends upon the rate at which adsorbate molecules diffuse toward the adsorbent surface [58]. The Avrami model determines some kinetic parameters, as possible changes to the adsorption rates in function of the initial concentration and the adsorption time, as well as the determination of fractional kinetic orders [59]. All kinetic parameters obtained from the fitting of the adsorption kinetic models are presented in Table 2.

According to the analysis of R^2 values, pseudo-second-order model is the most suitable one to describe the kinetics of MB adsorption on the Schiff bases. This indicates that the rate-determining step of the adsorption process may be a chemical sorption one involving valence forces through sharing or exchange of electrons between adsorbent and adsorbate [50,54,56]. In other words, the rate of the adsorption process depends upon the availability of the active adsorption sites rather than the adsorbate concentration in the bulk solution [60].

The high correlation coefficient R^2 values of the Avrami model cannot be neglected, indicating that the adsorption mechanism could follow many stages of several kinetic orders that are altered during the adsorbate–adsorbent contact [36,60]. Intraparticle diffusion mechanism seems to take part in the adsorption process.

From the aforementioned results, one can conclude that the adsorption process in our systems is somehow complicated.

Table 1
Adsorption parameters obtained from Freundlich and Langmuir models for MB adsorption on the Schiff bases

Sample	Freundlich			Langmuir		
	K_F (mg/g)(L/g)$^{1/n}$	n_F	R^2	K_L	q_{max}	R^2
Schiff base I	4.0695	1.5685	0.9807	3.6126	52.7899	0.7188
Schiff base II	5.0401	2.4696	0.983	4.2872	27.8925	0.8776
Schiff base III	5.4178	2.0538	0.9994	5.6967	36.6494	0.9379

Table 2
Different kinetic parameters for MB adsorption on the Schiff bases

Sample	Pseudo-first-order			Pseudo-second-order			Intraparticle diffusion		Avrami		
	k_1 (min^{-1})	q_e (mg/g)	R^2	k_2 (g/mg/min)	q_e (mg/g)	R^2	k_i (mg/g/min$^{0.5}$)	R^2	k_{AV} (min^{-1})	n_{AV}	R^2
Schiff base I	0.0501	3.6084	0.7355	0.0048	14.7929	0.9970	1.9820	0.9838	0.0940	1.0080	0.9978
Schiff base II	0.0128	2.7684	0.6757	0.0064	10.9938	0.9968	0.9701	0.9472	0.0486	0.7159	0.9910
Schiff base III	0.0104	3.0618	0.5781	0.0047	11.0607	0.9995	0.8513	0.9302	0.0346	0.7537	0.9971

4. Conclusions

Novel O-amine functionalized chitosan Schiff bases were developed by the coupling of O-amine functionalized chitosan with 4-methoxy benzaldehyde (Schiff base (I)), 4-chloro benzaldehyde (Schiff base (II)), and diethylamino acetone (Schiff base (III)) for the adsorption of cationic dye (MB) from aqueous solutions. Characteristic results show marked changes in their properties. The chemical structure was confirmed by FTIR analysis. The morphological analysis was studied by SEM and exhibits higher roughness and porosity of the surface. The optimum adsorption results show that the optimum adsorption time is 40, 120, and 180 min for Schiff bases (I), (II), and (III), respectively; The favorite adsorption pH is at neutral and alkaline pH. Furthermore, the results show a linear increase in the removing capacity of polymers with increasing the initial dye concentration to reach 35.6, 25.8, and 30.5 mg/g for Schiff bases (I), (II), and (III), respectively. Freundlich model was able to describe the equilibrium data and fitted perfectly. The experimental kinetics data clearly depict that the pseudo-second-order model is the most suitable one to represent the kinetics of the MB dye removal using the O-amine functionalized chitosan Schiff bases.

Competing interests

The authors declare that they have no competing interests.

Author's contributions

Authors have made equal contributions in conducting scientific researches and writing this paper. All authors read and approved the final manuscript.

Acknowledgment

Authors acknowledge the support of City of Scientific Research and Technological Applications (SRTA-City).

Funding

Authors have not used any external sources of funding in addition to regular financing for scientific investigations provided by City of Scientific Research and Technological Applications (SRTA-City).

References

[1] G.M. Walker, L. Hansen, J.A. Hana, S.J. Allen, Kinetics of a reactive dye adsorption onto dolomitic sorbents, Water Res., 37 (2003) 2081–2089.
[2] Q. Sun, L. Yang, The adsorption of basic dyes from aqueous solution on modified peat–resin particle, Water Res., 37 (2003) 1535–1544.
[3] A. Tor, Y. Cengeloglu, Removal of congo red from aqueous solution by adsorption onto acid activated red mud, J. Hazard. Mater., 138 (2006) 409–415.
[4] G. Bayramoglu, B. Altintas, M.Y. Arica, Synthesis and characterization of magnetic beads containing aminated fibrous surfaces for removal of Reactive Green 19 dye: kinetics and thermodynamic parameters, J. Chem. Technol. Biotechnol., 87 (2012) 705–713.
[5] G. Bayramoglu, M.Y. Arica, Preparation of comb-type magnetic beads by surface-initiated ATRP: modification with nitrilotriacetate groups for removal of basic dyes, Ind. Eng. Chem. Res., 51 (2012) 10629−10640.
[6] G. Bayramoglu, M.Y. Arica, Removal of reactive dyes from wastewater by acrylate polymer beads bearing amino groups: isotherm and kinetic studies, Color. Technol., 129 (2013) 114–124.
[7] C.H. Weng, Y.T. Lin, D.Y. Hong, Y.C. Sharma, S.C. Chen, K. Tripathi, Effective removal of copper ions from aqueous solution using base treated black tea waste, Ecol. Eng., 67 (2014) 127–133.
[8] D. Gusain, F. Bux, Y.C. Sharma, Abatement of chromium by adsorption on nanocrystalline zirconia using response surface methodology, J. Mol. Liq., 197 (2014) 131–141.
[9] S. Yadav, V. Srivastava, S. Banerjee, F. Gode, Y.C. Sharma, Studies on the removal of nickel from aqueous solutions using modified riverbed sand, Environ. Sci. Pollut. Res. Int., 20 (2013) 558–567.
[10] Y.C. Sharma, Uma, S.N. Upadhyay, An economically viable removal of methylene blue by adsorption on activated carbon prepared from rice husk, Can. J. Chem. Eng., 82 (2011) 377–383.
[11] S. Gopi, P. Balakrishnan, A. Pius, S. Thomas, Chitin nanowhisker (ChNW)-functionalized electrospun PVDF membrane for enhanced removal of Indigo carmine, Carbohydr. Polym., 165 (2017) 115–122.
[12] A. Naghizadeh, M. Ghafouri, A. Jafari, Investigation of equilibrium, kinetics and thermodynamics of extracted chitin from shrimp shell in reactive blue 29 (RB-29) removal from aqueous solutions, Desal. Wat. Treat., 70 (2017) 355–363.
[13] H.S. Kas, Chitosan: properties, preparations and application to microparticulate systems, J. Microencapsul., 14 (1997) 689–711.
[14] P.K. Dutta, J. Dutta, V.S. Tripathi, Chitin and chitosan: chemistry, properties and applications, J. Sci. Ind. Res., 63 (2004) 20–31.
[15] E.M. El-Sayed, T.M. Tamer, A.M. Omer, M.S. Mohy Eldin, Development of novel chitosan Schiff base derivatives for cationic dye removal: methyl orange model, Desal. Wat. Treat., 57 (2016) 22632–22645.
[16] M.S. Mohy Eldin, E.A. Soliman, A.I. Hashem, T.M. Tamer, Antibacterial activity of chitosan chemically modified with new technique, Trends Biomater. Artif. Organs, 22 (2008) 121–133.
[17] M.S. Mohy Eldin, E.A. Soliman, A.I. Hashem, T.M. Tamer, M.M. Sabet, Antifungal Activity of Aminated Chitosan Against Three Different Fungi Species (Chapter 26), In: D. Balköse, D. Horak, L. Šoltés, Eds., Key Engineering Materials-Current State-of the-Art on Novel Materials, vol. 1, 2013, pp. 415–431.
[18] M.S. Mohy Eldin, E.A. Soliman, A.I. Hashem, T.M. Tamer, Antimicrobial activity of novel aminated chitosan derivatives for biomedical applications, Adv. Polym. Technol., 31 (2012) 414–428.
[19] K. Valachová, T.M. Tamer, M.S. Mohy Eldin, L. Šoltés, Radical scavenging activity of glutathione, chitin derivatives and their combination, Chem. Pap., 70 (2016) 820–827.
[20] M.S. Mohy Eldin, A.M. Omer, M.A. Wassel, T.M. Tamer, M.S. Abd-Elmonem, S.A. Ibrahim, Novel smart pH sensitive chitosan grafted alginate hydrogel microcapsules for oral protein delivery: II. Evaluation of the swelling behavior., Int. J. Pharm. Pharm. Sci., 7 (2015) 331–337.
[21] A.M. Omer, T.M. Tamer, M.A. Hassan, P. Rychter, M.S. Mohy Eldin, N. Koseva, Development of amphoteric alginate/aminated chitosan coated microbeads for oral protein delivery, Int. J. Biol. Macromol., 92 (2016) 362–370.
[22] G. Tejada, G.N. Piccirilli, M. Sortino, C.J. Salomón, M.C. Lamas, D. Leonardi, Formulation and in-vitro efficacy of antifungal mucoadhesive polymeric matrices for the delivery of miconazole nitrate, Mater. Sci. Eng., C, 79 (2017) 140–150.
[23] I. Bano, M. Arshad, T. Yasin, M.A. Ghauri, M. Younus, Chitosan: a potential biopolymer for wound management, Int. J. Biol. Macromol., 102 (2017) 380–383.
[24] M.S. Chiou, H.Y. Li, Adsorption behavior of reactive dye in aqueous solution on chemical cross-linked chitosan beads, Chemosphere, 50 (2003) 1095–1105.

[25] M.S. Chiou, P.Y. Ho, H.Y. Li, Adsorption of anionic dyes in acid solutions using chemically cross-linked chitosan beads, Dyes Pigm., 60 (2004) 69–84.
[26] G. Annadurai, L.Y. Ling, J.F. Lee, Adsorption of reactive dye from an aqueous solution by chitosan: isotherm, kinetic and thermodynamic analysis, J. Hazard. Mater., 152 (2008) 337–346.
[27] G.L. Dotto, L.A.A. Pinto, Adsorption of food dyes acid blue 9 and food yellow 3 onto chitosan: stirring rate effect in kinetics and mechanism, J. Hazard. Mater., 187 (2011) 164–170.
[28] W.S.W. Ngah, L.C. Teong, M.A.K.M. Hanafiah, Adsorption of dyes and heavy metal ions by chitosan composites: a review, Carbohydr. Polym., 83 (2011) 1446–1456.
[29] H. Li, P. Wang, W. Liu, Removal of dibutyl phthalate (DBP) from aqueous solution by adsorption using vanillin-modified chitosan beads (CTSV), Desal. Wat. Treat., 56 (2015) 452–462.
[30] M. Mirabedini, M.Z. Kassaee, Removal of toxic Cr(VI) from water by a novel magnetic chitosan/glyoxal/PVA hydrogel film, Desal. Wat. Treat., 57 (2015) 14266–14279.
[31] G.Z. Kyzas, D.N. Bikiaris, Recent modifications of chitosan for adsorption applications: a critical and systematic review, Mar. Drugs, 13 (2015) 312–337.
[32] C.S. Thatte, M.V. Rathnam, A.C. Pise, Chitosan-based Schiff base-metal complexes (Mn, Cu, Co) as heterogeneous, new catalysts for the β-isophorone oxidation, J. Chem. Sci., 126 (2014) 727–737.
[33] E.A. Soliman, S.M. El-Kousy, H.M. Abd-Elbary, A.R. Abou-zeid, Low molecular weight chitosan-based Schiff bases: synthesis, characterization and antimicrobial activity, J. Food Technol., 8 (2013) 17–30.
[34] H.M.F. Freundlich, Über die adsorption in lösungen, Zeitschrift fur Physikalische Chemie, 57 (1906) 385–470.
[35] I. Langmuir, The constitution and fundamental properties of solids and liquids. Part I. Solids, J. Am. Chem. Soc., 38 (1916) 2221–2295.
[36] A.M.M. Vargas, A.L. Cazetta, M.H. Kunita, T.L. Silva, V.C. Almeida, Adsorption of methylene blue on activated carbon produced from flamboyant pods (*Delonix regia*): study of adsorption isotherms and kinetic models, Chem. Eng. J., 168 (2011) 722–730.
[37] Z.H. Wang, Y.L. Huang, The calculation of deacetylating degree of chitosan, J. Beijing Univ. Chem. Technol., 28 (2001) 84–86.
[38] A.M. Donia, A.A. Atia, K.Z. Elwakeel, Selective separation of mercury(II) using magnetic chitosan resin modified with Schiff's base derived from thiourea and glutaraldehyde, J. Hazard. Mater., 151 (2008) 372–379.
[39] Y. Liu, Y. Zheng, A. Wang, Enhanced adsorption of Methylene Blue from aqueous solution by chitosan-g-poly (acrylic acid)/ vermiculite hydrogel composites, J. Environ. Sci. (China), 22 (2010) 486–493.
[40] S. Chatterjee, T. Chatterjee, S.R. Lim, S.H. Woo, Adsorption of a cationic dye, methylene blue, on to chitosan hydrogel beads generated by anionic surfactant gelation, Environ. Technol., 32 (2011) 1503–1514.
[41] E. Assaad, A. Azzouz, D. Nistor, A.V. Ursu, T. Sajin, D.N. Miron, F. Monette, P. Niquette, R. Hausler, Metal removal through synergic coagulation–flocculation using an optimized chitosan–montmorillonite system, Appl. Clay Sci., 37 (2007) 258–274.
[42] A. Szyguła, E. Guibal, M.A. Palacın, M. Ruiz, A.M. Sastre, Removal of an anionic dye (Acid Blue 92) by coagulation-flocculation using chitosan, J. Environ. Manage., 90 (2009) 2979–2986.
[43] T.A. Arica, E. Ayas, M.Y. Arica, Magnetic MCM-41 silica particles grafted with poly(glycidylmethacrylate) brush: Modification and application for removal of basic dyes, Micropor. Mesopor. Mat., 243 (2017) 164–175.
[44] H. Hou, R. Zhou, P. Wu, L. Wu, Removal of Congo red dye from aqueous solution with hydroxyapatite/chitosan composite, Chem. Eng. J., 211–212 (2012) 336–342.
[45] G. Bayramoğlu, V.C. Ozalp, M.Y. Arıca, Removal of Disperse Red 60 as cationic dye from aqueous solution using free and entrapped fungus *Lentinus concinnus*, Water Sci. Technol., 75 (2017) 366–377.
[46] I. Uzun, Kinetics of the adsorption of reactive dyes by chitosan, Dyes Pigm., 70 (2006) 76–83.
[47] B. Noroozi, G.A. Sorial, H. Bahrami, M. Arami, Equilibrium and kinetic adsorption study of a cationic dye by a natural adsorbent – silkworm pupa, J. Hazard. Mater., 39 (2007) 167–174.
[48] D.M. Ruthven, Principles of Adsorption and Adsorption Processes, John Wiley & Sons, New York, 1984.
[49] S.M. Venkat, D.M. Indra, C.S. Vimal, Use of bagasse fly ash as an adsorbent for the removal of brilliant green dye from aqueous solution, Dyes Pigm., 73 (2007) 269–278.
[50] Y. Li, Y. Zhou, W. Nie, L. Song, P. Chen, Highly efficient methylene blue dyes removal from aqueous systems by chitosan coated magnetic mesoporous silica nanoparticles, J. Porous Mater., 22 (2015) 1383–1392.
[51] F. Marrakchi, W.A. Khanday, M. Asif, B.H. Hameed, Cross-linked chitosan/sepiolite composite for the adsorption of methylene blue and reactive orange 16, Int. J. Biol. Macromol., 93 (2016) 1231–1239.
[52] A.B. Albadarin, M.N. Collins, M. Naushad, S. Shirazian, G. Walker, C. Mangwandi, Activated lignin–chitosan extruded blends for efficient adsorption of methylene blue, Chem. Eng. J., 307 (2017) 264–272, doi: 10.1016/j.cej.2016.08.089.
[53] H. Yang, A. Sheikhi, G.M. Theo, Reusable green aerogels from cross-linked hairy nanocrystalline cellulose and modified chitosan for dye removal, Langmuir, 32 (2016) 11771–11779.
[54] Y. Zhang, X. Lin, Q. Zhou, X. Luo, Fluoride adsorption from aqueous solution by magnetic core-shell Fe_3O_4@alginate-La particles fabricated via electro-coextrusion, Appl. Surf. Sci., 389 (2016) 34–45.
[55] V. Dhanapal, K. Subramanian, Modified chitosan for the collection of reactive blue 4, arsenic and mercury from aqueous media, Carbohydr. Polym., 117 (2015) 123–132.
[56] H.Y. Zhu, Y.Q. Fu, R. Jiang, J. Yao, L. Xiao, G.M. Zeng, Novel magnetic chitosan/poly (vinyl alcohol) hydrogel beads: preparation, characterization and application for adsorption of dye from aqueous solution, Bioresour. Technol., 105 (2012) 24–30.
[57] W.J. Weber, J.C. Morris, Kinetics of adsorption carbon from solutions, P. Am. Soc. San. Eng., 89 (1963) 31–59.
[58] M.M. El-Zawahry, F. Abdelghaffar, R.A. Abdelghaffar, A.G. Hassabo, Equilibrium and kinetic models on the adsorption of Reactive Black 5 from aqueous solution using *Eichhornia crassipes*/chitosan composite, Carbohydr. Polym., 136 (2016) 507–515.
[59] C.E. Zubieta, P.V. Messina, C. Luengo, M. Dennehy, O. Pieroni, P.C. Schulz, Reactive dyes remotion by porous TiO_2-chitosan materials, J. Hazard. Mater., 152 (2008) 765–777.
[60] G.M.S. ElShafei, I.M.A. ElSherbiny, A.S. Darwish, C.A. Philip, Silkworms' feces-based activated carbons as cheap adsorbents for removal of cadmium and methylene blue from aqueous solutions, Chem. Eng. Res. Des., 92 (2014) 461–470.